41. 厚生労働省医薬食品局長.「血液製剤等に係る遡及調査ガイドライン」の一部改正について. 薬食発第1226008号, 薬食発第1226009号, 薬食発第1226010号, 薬食発第1226011号. 平成20年12月26日

42. 厚生省医薬安全局審査管理課長.「ヒト又は動物細胞株を用いて製造されるバイオテクノロジー応用医薬品のウイルス安全性評価」について. 医薬審第329号 平成12年2月22日

Analytical Biochemistry 420 (2012) 61–67

Contents lists available at SciVerse ScienceDirect

Analytical Biochemistry

journal homepage: www.elsevier.com/locate/yabio

Analysis of oligomeric stability of insulin analogs using hydrogen/deuterium exchange mass spectrometry

Shiori Nakazawa [a,b], Noritaka Hashii [a,*], Akira Harazono [a], Nana Kawasaki [a,b]

[a] Division of Biological Chemistry and Biologicals, National Institute of Health Sciences, 1–18–1 Kami-yoga, Setagaya-ku, Tokyo 158-8501, Japan
[b] Graduate School of Life Science, Hokkaido University, Kita 12-Nishi 6, Kita-ku, Sapporo 060-0812, Japan

ARTICLE INFO

Article history:
Received 8 July 2011
Received in revised form 9 August 2011
Accepted 1 September 2011
Available online 7 September 2011

Keywords:
Insulin
HDX/MS
Oligomeric stability

ABSTRACT

Insulin analog products for subcutaneous injection are prepared as solutions in which insulin analog molecules exist in several oligomeric states. Oligomeric stability can affect their onset and duration of action and has been exploited in designing them. To investigate the oligomeric stability of insulin analog products having different pharmacokinetics, we performed hydrogen/deuterium exchange mass spectrometry (HDX/MS), which is a rapid method to analyze dynamic aspects of protein structures. Two rapid-acting analogs (lispro and glulisine) incorporated deuteriums more and faster than recombinant human insulin, whereas a long-acting analog (glargine) and two intermediate-acting preparations (protamine-containing formulations) incorporated them less and more slowly. Kinetic analysis revealed that the number of slowly exchanged hydrogens (D_s) ($k < 0.01\ min^{-1}$) accounted for the difference in HDX reactivity among analogs. Furthermore, we found correlations between HDX kinetics and pharmacokinetics reported previously. Their maximum serum concentration (C_{max}) was linearly correlated with D_s ($r = 0.88$) and the number of maximum exchangeable hydrogens (D_∞) ($r = 0.89$). The maximum drug concentration time (t_{max}) was also correlated with reciprocals of D_s and D_∞ ($r = 0.86$ and $r = 0.96$, respectively). Here we demonstrate the ability of HDX/MS to evaluate oligomeric stability of insulin analog products.

Insulin is a peptide hormone consisting of two peptides: an A chain with 21 amino acids and a B chain with 30 amino acids. Insulin is the only hormone in vertebrates to induce cellular uptake of glucose and lower blood glucose levels, and it is an essential drug for treating diabetes mellitus.

As a drug product, insulin molecules primarily form hexamers, which diffuse and dilute in the subcutaneous tissue after injection [1] and dissociate into monomers via dimers or tetramers [1,2]. Monomeric insulin is absorbed into microvessels to exert its pharmacological action [3]. Therefore, oligomeric stability is a crucial property of insulin, determining its onset and duration of action (Fig. 1).

To mimic the intrinsic insulin secretion and enable better control of blood glucose levels, several recombinant human insulin analogs with different onset and duration of action have been developed and marketed. Compared with the basic preparation of recombinant human insulin, insulin analog products are generally categorized on the basis of differences in the onset and duration of their action—rapid-acting, long-acting, and intermediate-acting groups. Fig. 2 and Table 1 present the primary structures and several characteristics of insulin analogs investigated in this study [4–6]. Insulin lispro (lispro) is a rapid-acting insulin analog in which the positions of proline at B28 and lysine at B29 are reversed. Insulin glulisine (glulisine) is another major rapid-acting analog in which asparagine and lysine at positions B3 and B29 are replaced by lysine and glutamic acid, respectively. The amino acid substitutions in lispro and glulisine lead to a decrease in oligomeric stability; therefore, they act rapidly after subcutaneous injection. Insulin glargine (glargine) is a long-acting analog in which asparagine at position 21 on the A chain is substituted by glycine and two arginine residues are added to the C terminus of the B chain. Glargine has a higher isoelectric point (6.7) [7,8] than human insulin and its analogs, which range from 5.0 to 5.5 [9–12]. Glargine formulated at pH 3.5 to 4.5 precipitates in neutral conditions after subcutaneous injection [13,14]. Its precipitant gradually dissociates and is absorbed slowly into the bloodstream, and thereby glargine has a slower onset and longer duration of action than human insulin. Insulin detemir (detemir) is another type of long-acting analog that was designed with a concept different from modification of oligomeric stability. Detemir, in which a myristic acid is covalently bound to lysine at B29, binds to albumin in subcutaneous tissues and plasma. This modification leads to delay in absorption and prolongation of the serum half-life. The intermediate-acting group is another type of insulin with longer action in which the hexameric insulin (analog) is stabilized by forming a

* Corresponding author. Fax: +81 3 3700 9084.
E-mail address: hashii@nihs.go.jp (N. Hashii).

0003-2697/$ - see front matter © 2011 Elsevier Inc. All rights reserved.
doi:10.1016/j.ab.2011.09.002

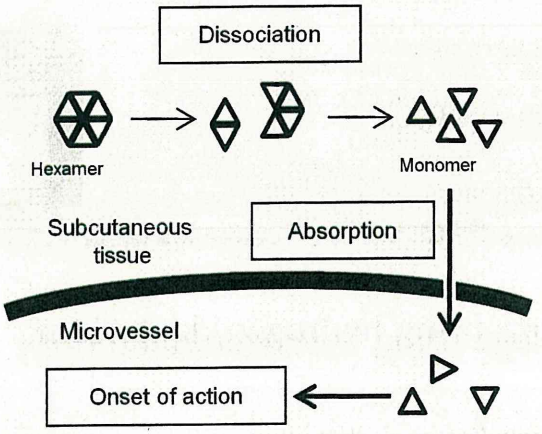

Fig.1. Absorption of subcutaneously injected insulin. Insulin molecules in drug products exist mainly as hexamers. After subcutaneous injection, diluted hexamers dissociate to monomers to be absorbed by microvessels.

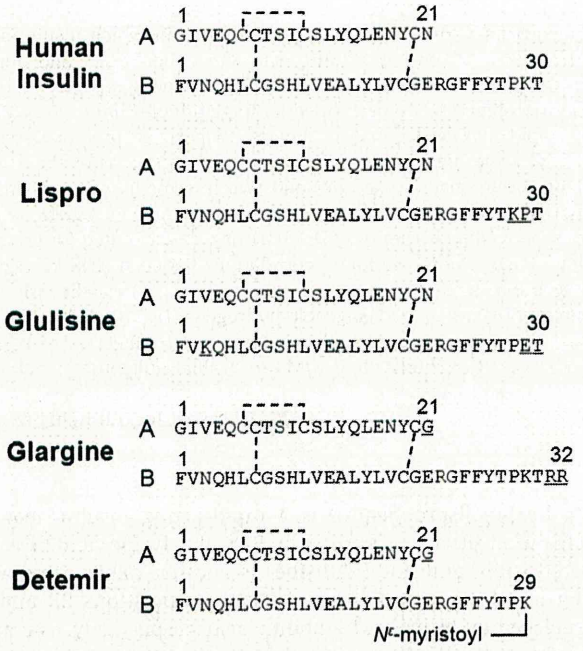

Fig.2. Primary structures of insulin analogs we examined. Dashed lines represent disulfide bonds. Mutated residues are underscored.

Table 1
Human insulin and its analog products examined in this study.

Group	Analog	Onset of action	Duration of action	Molecular weight	*pI*	pH of drug product
	Human Insulin	30–60 min	4–12 h	5807.57	5.4	7.0–7.8
Rapid	Lispro	5–15 min	4–6 h	5807.57	5.65	7.0–7.8
	Glulisine	5–15 min	1–2.5 h	5822.58	5.1	7.0–7.8
Long	Glargine	2–4 h	20–24 h	6062.89	6.7	3.5–4.5
	Detemir	2 h[a]	6–24 h[a]	5916.82		7.2–7.6
Intermediate	NPH	2–4 h	10–16 h	5807.57		7.0–7.5
	NPL	1–2 h	10–16 h	5807.57		7.0–7.8

[a] Dose dependent.

complex with protamine to suppress dissociation in subcutaneous tissue after injection. Human isophane insulin (neutral protamine Hagedorn, NPH)[1] and a lispro preparation containing protamine (neutral protamine lispro, NPL) belong to the intermediate-acting group.

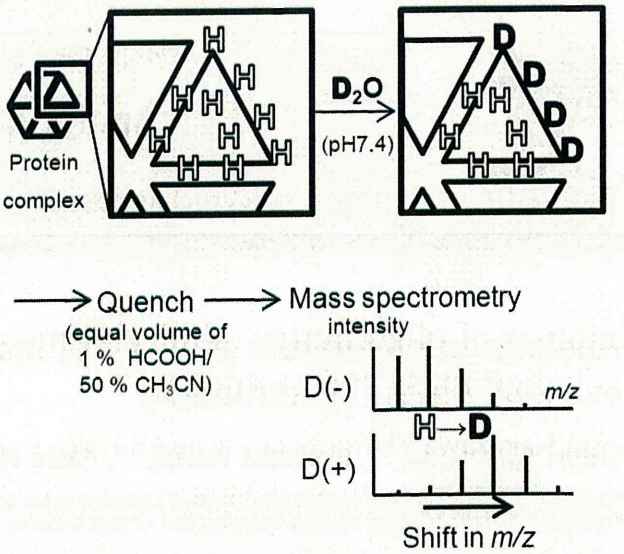

Fig.3. Schematic model of HDX/MS. The protein sample is exposed to deuterated solvent and subjected to MS. Hydrogen atoms, without participating in hydrogen bonds or any other noncovalent bonds, are more easily exchanged with deuteriums. Exchanged deuteriums are detected as the shift in *m/z* value distributions.

Evaluation of oligomeric states of formulated insulin analogs is important to support their appropriate use. Previously, the oligomeric states of insulin analogs were determined by sedimentation velocity or static light scattering or were estimated by comparing their circular dichroism spectra under different conditions [15]. However, the oligomeric stability of these formulated insulin analogs have not been investigated because of the absence of convenient methods. Therefore, there is an increasing need for an easy, rapid, and accurate method to evaluate stability of the association state of insulin.

Hydrogen/deuterium exchange mass spectrometry (HDX/MS) is a known method to analyze structural fluctuations of proteins [16–18]. HDX/MS is based on the exchange reaction between hydrogens in proteins and deuteriums in the D_2O solvent. A protein sample is incubated in a D_2O solvent to incorporate deuteriums, and then the sample solution is mixed with an acidic reagent to suppress the HDX reaction. The number of incorporated deuteriums is calculated from the difference in the average mass obtained by liquid chromatography mass spectrometry (LC/MS) before and after the HDX reaction (Fig. 3). Deuteriums that were exchanged with amide hydrogens in the protein backbone are primarily detected by HDX/MS because hydrogens in protein side chain groups (e.g., –OH, $–NH_2$, –SH, –COOH, $–CONH_2$) have lower pK_a values, have higher exchange rates even after the addition of H^+, and undergo a back-exchange reaction to lose deuteriums [19]. The exchange rate of each amide hydrogen depends on its interaction with the solvent [20–22]. A moiety with more structural fluctuations, which is not involved in an α-helix or a β-sheet, not packed in the hydrophobic core, and not trapped in other interactions, has more solvent accessibility. Thus, a moiety or molecule that interacts with the solvent further (e.g., a monomer vs. an oligomer) will gain more exchanged deuteriums [23].

[1] *Abbreviations used:* NPH, neutral protamine Hagedorn; NPL, neutral protamine lispro; HDX/MS, hydrogen/deuterium exchange mass spectrometry; LC/MS, liquid chromatography mass spectrometry; HPLC, high-performance liquid chromatography; PCA, principal component analysis; DSL, dynamic light scattering.

HDX/MS can potentially be applied to estimate the stability of insulin oligomers.

In this study, we compared the HDX reactivity of insulin analog formulations with different oligomeric stability and different drug dispositions. We found correlations between their HDX kinetic parameters and their pharmacokinetic parameters. Here we demonstrate the usefulness of HDX/MS to evaluate oligomeric stability of insulin analog products and propose its potential use for predicting their onset and duration of action.

Materials and methods

Materials

Human insulin (Humulin R), insulin lispro (Humalog), NPH insulin (Humulin N), and NPL (Humalog N) were purchased from Eli Lilly (Indianapolis, IN, USA). Insulin glargine (Lantus) and insulin glulisine (Apidra) were purchased from Sanofi–Aventis (Paris, France). Insulin detemir (Levemir Penfill) was purchased from Novo Nordisk (Bagsværd, Denmark). All compounds were provided at a concentration of 100 U/ml, approximately 3.5 mg/ml (0.61 mM). Ammonium acetate and formic acid were purchased from Wako Pure Chemical Industries (Osaka, Japan). Acetonitrile and D_2O were purchased from Sigma–Aldrich (St. Louis, MO, USA).

HDX/MS

Protein solutions were diluted 10-fold with 10 mM ammonium acetate in 90% D_2O (pH 7.4) and kept on ice during the HDX reaction because conducting the reaction at room temperature resulted in a very high exchange rate that made it difficult to successfully observe a time-dependent change. Final concentrations of insulin analogs were approximately 60 mM (0.35 mg/ml). At each time point, 50 µl of the reaction solution was mixed with an equal volume of ice-chilled formic acid/acetonitrile/water (1:49:50) to repress the exchange reaction; this step is called "quenching." Deuterated proteins were introduced into the mass spectrometer with the Paradigm MS4 HPLC (high-performance liquid chromatography) system (Michrom BioResoruces, Auburn, CA, USA) through an L-column Micro trap column with C18 solid phase (Chemicals Evaluation and Research Institute, Tokyo, Japan) at a flow rate of 50 µl/min over 10 min with 0.1% formic acid in 50% acetonitrile. Mass spectra were recorded using a Fourier transform ion cyclotron resonance mass spectrometer (LTQ-FT, Thermo Fisher Scientific, Waltham, MA, USA) equipped with a nanoelectrospray ion source (AMR, Tokyo, Japan). The conditions for MS analysis were as follows: an electrospray voltage of 2.5 kV in positive ion mode, a capillary temperature of 200 °C, and an m/z range of 1000 to 4000. The number of incorporated deuteriums was determined by subtraction of the weight-average molecular weights.

Table 2
Hydrodynamic diameters of insulin analogs in 10 mM ammonium acetate (pH 7.4).

	Concentration (µM)			
	15	30	60	120
Insulin	4.7 ± 0.1	5.1 ± 0.3	4.7 ± 0.1	4.6 ± 0.1
Lispro	3.2 ± 0.4	3.6 ± 0.6	4.4 ± 0.2	4.6 ± 0.1
Glulisine	3.3 ± 0.6	3.7 ± 0.2	4.5 ± 0.1	4.5 ± 0.3
Glargine	609.1 ± 42.8	284.2 ± 8.2	274.0 ± 28.0	4.9 ± 0.1
Detemir	13.2 ± 0.1	11.0 ± 2.9	6.2 ± 0.0	5.4 ± 0.1
Insulin/H^+			2.6 ± 1.0	

Note. Values are mean diameters (nm) ± standard deviations ($n = 3$).

Table 3
Relative volume in neutral buffer compared with that of human insulin in acidic solution.

	Concentration (µM)			
	15	30	60	120
Insulin	5.9	7.6	6.2	5.8
Lispro	1.9	2.8	5.1	5.5
Glulisine	2.1	2.9	5.4	5.3
Glargine	1.3×10^7	1.3×10^6	1.2×10^6	6.8
Detemir	131.6	77.2	14.0	9.2

Note. Relative volume (to insulin/H^+) was calculated as (mean diameter of each analog at each concentration)^3/(mean diameter of insulin/H^+)^3.

Table 4
HDX kinetics of insulin analogs.

	Number of exchangeable hydrogens				
	Maximum (D_∞)	(D_0)	Slow (D_s)	Medium (D_i)	Fast (D_f)
Insulin	20.3	(11.9)	3.9	1.5	3.0
Lispro	24.5	(12.2)	7.3	2.6	2.5
Glulisine	24.7	(12.1)	7.2	2.6	2.8
Glargine	18.0	(10.1)	2.0	1.8	4.2
Detemir	19.9	(12.7)	3.3	1.6	2.5
NPH	16.4	(9.9)	1.0	1.8	3.6
NPL	16.9	(11.8)	1.3	2.0	1.8

Note. Shown are numbers of maximum exchangeable hydrogens and slow-exchanging ($k \leq 0.1\ min^{-1}$), intermediate-exchanging ($0.1 < k \leq 1$), or fast-exchanging ($k > 1.0$) hydrogens that were calculated on the basis of Eq. (1). D_t values of when $t = 0$ are in parentheses.

Calculation of kinetic parameters

The modeling and calculation of deuterium incorporation were done using Mathcad 14.0 software (PTC, Needham, MA, USA). Details of fitting with Eq. (1) are described in Results.

Size distribution measurements

Hydrodynamic diameter distributions were determined with the dynamic light scattering method by Zetasizer Nano (Malvern Instruments, Worcestershire, UK). Insulin analog products were diluted with 10 mM ammonium acetate (pH 7.4) to 15, 30, 60, and 120 µM. Acidic solution of insulin for the control was prepared with Humulin R and a 9-fold volume of 0.1% formic acid, which had a final pH of 2.7 at 25.7 °C. Overnight equilibration was performed at 4 °C prior to measurements. The relative volume given in Table 3 was calculated as the cube of the ratio of the mean diameter to that of insulin/H^+.

Multivariate analysis

Principal component analysis (PCA) was performed using SIMCA-P$^+$ software (Umetrics, Umeå, Sweden) with the PCA method. As the variables, the numbers of maximum exchangeable hydrogens (D_∞), and slow- and intermediate-exchanging hydrogens (D_s and D_i, respectively) (Table 4) were input. Before input, the variables were divided by the number of amide hydrogens in the main chains of each analog.

Results

Hydrodynamic diameter distributions of insulin analog products

To confirm the oligomeric states of insulin analogs used in this study, the particle size of four analogs (lispro, glulisine, glargine, and detemir) were measured by dynamic light scattering (DLS) after dilution of these analogs with an H_2O solvent of the same

composition as HDX solvent (Tables 2 and 3). As a control, an acidic solution of 60 μM human insulin (insulin/H^+), in which insulin exists mainly as a mixture of monomers and dimers, was prepared [24]. At a high concentration (120 μM), the mean diameters of the four analogs obtained by DLS were similar to that of human insulin. In addition, their volumes calculated from the mean diameters were 6-fold larger than that of insulin/H^+ (Table 3), suggesting that they could exist as hexamers at a high concentration.

At lower concentrations (15 and 30 μM), the mean diameters of the two rapid-acting analogs, lispro and glulisine, were smaller than the diameters at higher concentrations, although the diameter of human insulin remained roughly constant at all concentrations. These data indicate that the rapid-acting analogs dissociate more rapidly than human insulin. Glargine, with an isoelectric point of 6.7, showed an increase in diameter with a decrease in concentration by dilution with a neutral solvent, indicating the aggregation of glargine molecules. At lower concentrations (15 μM), detemir formed large particles approximately 130 times larger than insulin/H^+, possibly suggesting the association of detemir molecules at lower concentrations. These results are consistent with the prevailing oligomeric stability of insulin analogs except for detemir.

HDX/MS of human insulin and insulin analogs

First, to determine deuterium incorporation by human insulin as the standard, human insulin was subjected to the HDX reaction and LC/MS as described in Materials and Methods. To conduct exchange reaction under physiological pH conditions, we selected ammonium acetate buffer, one of the better buffers to mimic in vivo pH condition, considering applicability to the mass spectrometer. The time-dependent shift of the mass spectra and the number of incorporated deuteriums by human insulin are shown in Figs. 4 and 5 (red rhombus). The uptake was fast during the first 5 min, and approximately 80% of the incorporation was complete within the first minute. After 3 h of the HDX reaction, the number of incorporated deuteriums was 19.82 ± 1.64 (mean ± standard deviation, $n = 4$).

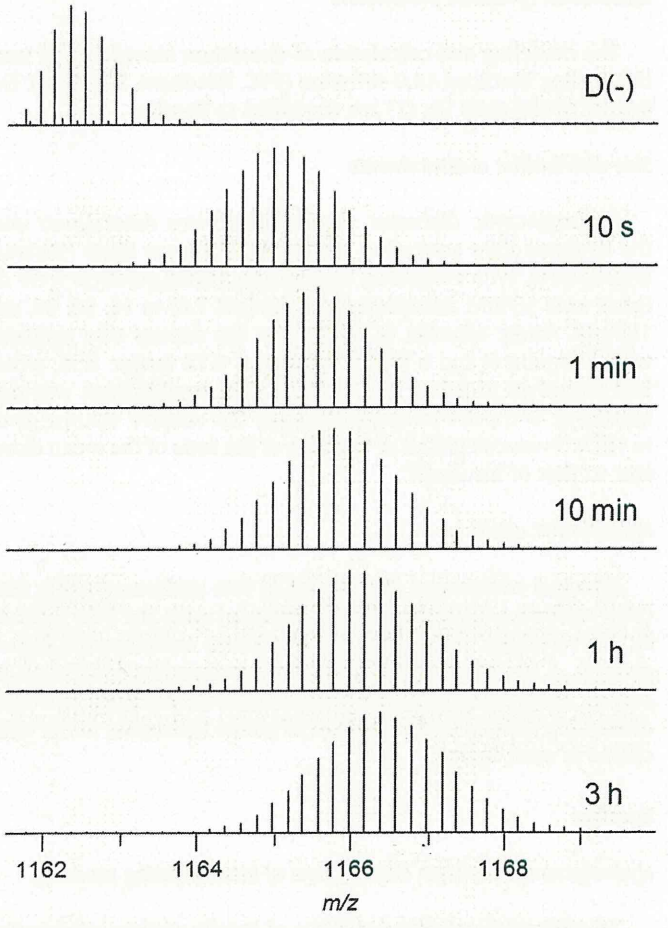

Fig.4. Representative mass spectra of human insulin observed during the HDX procedure. The original spectrum of human insulin without deuterium label [D(−)] and spectra obtained at several time points of HDX reaction are shown.

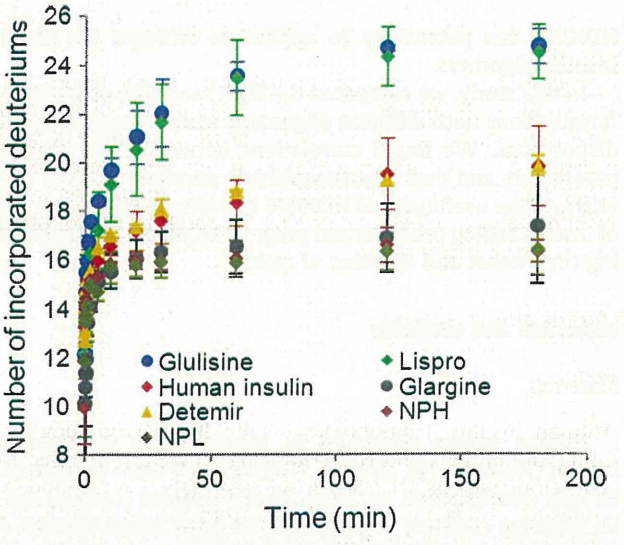

Fig.5. Time-series plot of deuterium uptake by insulin analog products.

Next, to determine whether the HDX reactivity of rapid-, long-, or intermediate-acting insulin analogs differed from that of human insulin, six analog products were examined (Fig. 5). Lispro and glulisine exhibited higher exchange reactivity than human insulin (24.48 ± 1.10 and 24.74 ± 0.70, respectively, after a 3 h reaction, $n = 3$), but glargine showed lower exchange reactivity than human insulin (17.57 ± 0.42 after 3 h, $n = 3$), indicating its enhanced oligomeric stability. Similarly, two formulations of the intermediate-acting group, NPH and NPL, also had lower reactivity (16.32 ± 0.43 and 16.39 ± 1.03, respectively, after 3 h, $n = 3$). Unlike the other analogs, detemir had a similar number of incorporated deuteriums as human insulin (19.84 ± 0.40 after 3 h, $n = 3$).

Kinetics of HDX reactivity of insulin analogs

To obtain further information on the oligomeric stability of insulin analogs, we investigated the kinetics of HDX reactions of human insulin and the insulin analogs. In general, HDX reactions of proteins can be modeled as a pseudo-first-order reaction [21], and exchangeable amide hydrogens are classified into three kinetic groups: fast-, intermediate-, and slow-exchanging hydrogens [25]. On these bases, we calculated the kinetics using Eq. (1), a tetranomial function of reaction time (t) defined by reaction rate constants of each hydrogen group (k_f, k_i, and k_s), denoting the maximum number of exchangeable hydrogen atoms by D_∞, and the number of hydrogens of each kinetic group by D_f, D_i, and D_s. The latter three terms represent the hydrogens that have not been exchanged after a t-min reaction. We employed the tetranomial model because it gave higher values of Pearson correlation coefficients than modeling with three or five terms:

$$D_t = D_\infty - D_f \exp(-k_f t) - D_i \exp(-k_i t) - D_s \exp(-k_s t). \quad (1)$$

The sets of coefficients (D_f, D_i, D_s, and D_∞) and reaction rate constants (k_f, k_i, and k_s) that gave the highest Pearson correlation coefficients were sought by fitting the mean number of incorporated

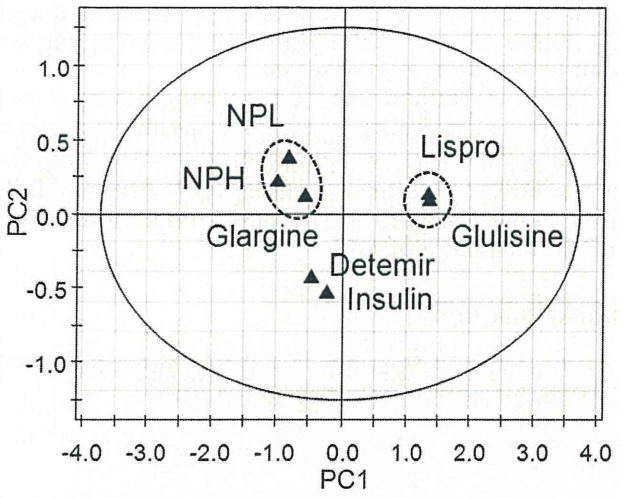

Fig.6. The score plot for the PCA of the HDX kinetic parameters. Primary (PC1) and secondary (PC2) principal components are indicated.

Table 5
Reported values of C_{max} and t_{max}.

Analog	C_{max} (μU/ml)	t_{max} (min)	Reference
Insulin	43.3	109	[26]
	35.8	97.5	[27]
	40.0	104	[28]
	46.0	92	[28]
	46.0	82	[29]
	51.1	101	[11]
Lispro	147.2	71	[30]
	81.0	71	[28]
	91.4	53	[11]
Glulisine	73.0	57	[28]
	92.0	83	[28]
	82.0	55	[29]
Glargine	18.9	180	[31]
NPH	13.5		[32]
	20.0		[32]
	22.8	360	[31]
NPL	21.3	200	[30]

Note. Shown are reported values of C_{max} and t_{max} in studies about insulin analog products [11,26–32]. Glargine's t_{max} was deduced from the time–concentration plot in Ref. [31].

deuteriums at every observed time point to Eq. (1). The resulting values for D_f, D_i, D_s, and D_∞ are shown in Table 4. The fast-acting group had the highest D_∞, followed by the human insulin, long-acting, and intermediate-acting groups. Interestingly, the number of hydrogens that were already exchanged at the beginning of the HDX reaction (D_t when $t = 0$) was not different among the respective groups, suggesting that differences in D_∞ originated from hydrogens that had lower exchange reaction rates and, therefore, were not exchanged during the first few seconds. Furthermore, D_s of the rapid-acting analogs were increased compared with those of the other groups. From these results, the number of D_s could be related to the difference in the overall HDX reactivity among insulin analogs.

PCA using HDX kinetic parameters of insulin analogs

We examined whether rapid-, long-, and intermediate-acting groups were distinguished by PCA using the HDX kinetic parameters, D_∞, D_f, D_i, and D_s. The score plots for PC1 and PC2 are shown in Fig. 6. Lispro and glulisine were plotted at neighboring positions, distant from human insulin and other analogs. In addition, three preparations with a lower tendency for dissociation (i.e., glargine, NPH, and NPL) were plotted closely together. However, detemir was plotted near human insulin, not near analogs of the long-acting group. This result demonstrates that the insulin analogs with different pharmaceutical properties are distinguished by their HDX reactivity.

Pharmacokinetic parameters and HDX kinetics of insulin analogs

We analyzed the association between the HDX kinetic parameters and the actual pharmacokinetic parameters in humans. We compared previously reported values [11,26–32] of the maximum plasma concentrations (C_{max}) and the maximum drug concentration time (t_{max}) after subcutaneous injection with our kinetic parameters, D_∞, D_s, D_i, and D_f (Table 5). Detemir, employing the affinity to albumin instead of the oligomeric stability for its longer action, was excluded. C_{max} had linear correlations with D_∞ and D_s ($r = 0.88$ and $r = 0.89$, respectively) (Fig. 7A). In addition, t_{max} correlated with reciprocals of D_∞ and D_s ($r = 0.86$ and $r = 0.96$, respectively) (Fig. 7B).

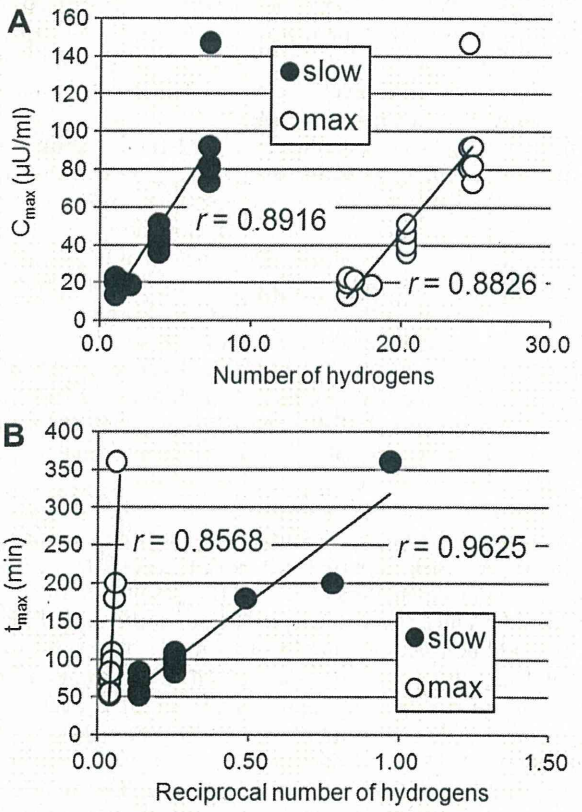

Fig.7. Relations between HDX kinetic parameters and C_{max} (A) or t_{max} (B) values.

Discussion

Since insulin lispro was first sold in 1995 as an analog of recombinant human insulin, many insulin analog products have been marketed. Oligomeric stability of formulated analogs is important for controlling their onset and duration of action. In this study, we analyzed the oligomeric stability of formulated insulin analogs by HDX/MS, which is an analytical method to determine structural fluctuations of proteins, and we investigated relationships between the parameters of HDX kinetics and pharmacokinetics of the analogs.

We first measured the diameters of the formulated insulin analogs under the same conditions as the HDX reaction. The diameters of two rapid-acting analogs (lispro and glulisine), which have low oligomeric stability, were smaller than that of human insulin at low concentrations, although glargine, a long-acting analog, formed large aggregates with an increase in pH by neutralization (Fig. 4). These results are consistent with previous studies and provide evidence that rapid-acting analogs dissociate more easily than human insulin and glargine forms aggregates at physiological pH. Detemir, another long-acting analog, exhibited unique behavior. It did not form huge aggregates like glargine, but it had larger diameters with dilution; its mean diameters were 2- or 3-fold larger than those of human insulin. This would have resulted from the suggested complex of detemir hexamers mediated by their acyl chains [33,34].

Next, we determined the HDX reactivity of human insulin and insulin analogs of rapid-, long-, and intermediate-acting groups (Fig. 5). Lispro and glulisine incorporated more deuteriums than human insulin. On the other hand, glargine and two products of the intermediate-acting group (NPH and NPL) incorporated fewer deuteriums than human insulin. These results demonstrate that HDX reactivity of insulin analogs at neutral pH were associated with their oligomeric stability. Interestingly, detemir, in spite of its prolonged action, had exchange reactivity similar to that of human insulin. Considering the mechanism in which detemir hexamers associate, there could be little effect on the solvent accessibility of peptide moieties of detemir molecules even when their hexamers form a larger complex.

The PCA using kinetic parameters of the HDX reactions resulted in a distinction among the three groups (Fig. 6). Two analogs of the rapid-acting group, one long-acting preparation, and two intermediate-acting preparations were plotted at close positions. However, detemir was plotted far from the other analogs of long- and intermediate-acting groups and was closer to human insulin. This result was in agreement with the time-dependent incorporation of deuteriums (Fig. 4). We suggest that only four kinetic parameters (D_∞, D_f, D_i, and D_s) obtained by HDX/MS allow for discrimination of insulin analogs of different groups. In addition, PCA using the kinetic parameters could also be applicable to evaluate similarities in similar biological medicinal products of insulin analogs under development.

We analyzed the association between the HDX kinetic parameters and the actual pharmacokinetic parameters in humans. We compared previously reported values of C_{max} and t_{max} (Table 5) with our kinetic parameters (Table 4). This resulted in the correlations with D_∞ and D_s shown in Fig. 7. These results suggest that D_∞ and D_s could be useful as characteristic markers for prediction of C_{max} and t_{max}. In a previous study on HDX with human insulin and lispro reported by Chitta and coworkers [25], D_∞ values were nearly equal to the total number ($D_f + D_i + D_s$) of amide deuteriums in the peptide backbone. However, in our study, the total number of D_f, D_i, and D_s was from 30% to 51% of D_∞, indicating that there could be some deuteriums left in side chains. Differences from the previous study could be caused by the difference in the temperature at which the HDX reaction was performed. In other words, continuous cooling through the entire procedure of HDX to moderate the exchange reaction in our study could account for the differences. Chitta and coworkers also reported a difference in D_i between human insulin and lispro [25], whereas in our study the only difference was observed in the D_s numbers. On ice, incubation could have switched some of the fast hydrogens to intermediate hydrogens and switched some of the intermediate hydrogens to slow hydrogens.

The concentration of insulin is a significant factor that affects the association and dissociation of insulin oligomer [24] and, thus, also affects the HDX reactivity [25]. When comparing the oligomeric stability of insulin preparations by HDX/MS, one should be careful about sample concentration because the difference in HDX reactivity could attenuate if insulin concentration were too high to dissociate (or too low to form even dimer).

Finally, we demonstrated the utility and capability of the HDX/MS method for evaluating the oligomeric stability of insulin analog products. We also revealed relationships between some HDX kinetic parameters and pharmacokinetic parameters. We believe that our current method could be helpful in predicting the pharmacokinetics of insulin analogs.

Acknowledgment

This study was supported in part by a Grant-in-Aid from the Ministry of Health, Labour, and Welfare (Japan).

References

[1] J. Brange, D.R. Owens, S. Kang, A. Volund, Monomeric insulins and their experimental and clinical applications, Diabetes Care 13 (1990) 923–954.
[2] M.R. DeFelippis, R.E. Chance, B.H. Frank, Insulin self-association and the relationship to pharmacokinetics and pharmacodynamics, Crit. Rev. Ther. Drug Carrier Syst. 18 (2001) 201–264.
[3] J. Brange, A. Volund, Insulin analogs with improved pharmacokinetic profiles, Adv. Drug Deliv. Rev. 35 (1999) 307–335.
[4] J.A. Mayfield, R.D. White, Insulin therapy for type 2 diabetes: rescue, augmentation, and replacement of beta-cell function, Am. Fam. Physician 70 (2004) 489–500.
[5] S.N. Charugulla, T.S. Kamat, K. Peetambaran, V.M. Thorat, Insulin analogues: an update, Res. J. Krishna Inst. Karad 2 (2009) 6–12.
[6] NIH Daily Med, HUMULIN (insulin human) injection, solution (Eli Lilly and Company). 2011. Available from: <http://dailymed.nlm.nih.gov/dailymed/druginfo.cfm?id=43212>.
[7] C. Binder, A theoretical model for the absorption of soluble insulin, in: P. Brunetti (Ed.), Artificial Systems for Insulin Delivery, Raven, New York, 1983, pp. 53–57.
[8] C.J. Dunn, G.L. Plosker, G.M. Keating, K. McKeage, L.J. Scott, Insulin glargine: an updated review of its use in the management of diabetes mellitus, Drugs 63 (2003) 1743–1778.
[9] O. Wintersteiner, H.A. Abramson, The isoelectric point of insulin, J. Biol. Chem. 99 (1993) 741–753.
[10] T. Blundell, G. Dodson, D. Hodgkin, D. Mercola, Insulin: the structure in the crystal and its reflection in chemistry and biology, Adv. Protein Chem. 26 (1972) 279–402.
[11] Eli Lilly Canada, Humalog product monograph. 2011. Available from: <http://www.lilly.ca/servlets/sfs;jsessionid=2606BA9CBC69DD8DCF6B024A9D13FEB9?t=/documentManager/sfdoc.file.supply&e=UTF-8&i=1233164768976&l=0&s=2S4REX2uNLETAStSC&fileID=1299285990234>.
[12] European Medicines Agency Committee for Medicinal Products for Human Use, Apidra: European Public Assessment Report—Scientific Discussion. 2011. Available from: <http://www.ema.europa.eu/ema/index.jsp?curl=pages/medicines/human/medicines/000557/human_med_000648.jsp&murl=menus/medicines/medicines.jsp&mid=WC0b01ac058001d125#>.
[13] G.B. Bolli, D.R. Owens, Insulin glargine, Lancet 356 (2000) 443–445.
[14] U. Dashora, V. Dashora, Insulin glargine, Int. J. Diabetes Dev. Countries 20 (2000) 140–144.
[15] D.L. Bakaysa, J. Radziuk, H.A. Havel, M.L. Brader, S. Li, S.W. Dodd, J.M. Beals, A.H. Pekar, D.N. Brems, Physicochemical basis for the rapid time–action of $Lys^{B28}Pro^{B29}$–insulin: dissociation of a protein–ligand complex, Protein Sci. 5 (1996) 2521–2531.
[16] A. Hvidt, K. Linderstrøm-Lang, Exchange of hydrogen atoms in insulin with deuterium atoms in aqueous solutions, Biochim. Biophys. Acta 14 (1954) 574–575.
[17] S.W. Englander, L. Mayne, Y. Bai, T.R. Sosnick, Hydrogen exchange: the modern legacy of Linderstrøm-Lang, Protein Sci. 6 (1997) 1101–1109.
[18] Y. Hamuro, S.J. Coales, M.R. Southern, J.F. Nemeth-Cawley, D.D. Stranz, P.R. Griffin, Rapid analysis of protein structure and dynamics by hydrogen/deuterium exchange mass spectrometry, J. Biomol. Tech. 14 (2003) 171–182.
[19] X. Yan, J. Watson, P.S. Ho, M.L. Deinzer, Mass spectrometric approaches using electrospray ionization charge states and hydrogen–deuterium exchange for determining protein structures and their conformational changes, Mol. Cell. Proteomics 3 (2003) 10–23.
[20] S.W. Englander, D.B. Calhoun, J.J. Englander, N.R. Kallenbach, R.K. Liem, E.L. Malin, C. Mandal, J.R. Rogero, Individual breathing reactions measured in hemoglobin by hydrogen exchange methods, Biophys. J. 32 (1980) 577–589.
[21] Z.Q. Zhang, D.L. Smith, Determination of amide hydrogen exchange by mass spectrometry: a new tool for protein structure elucidation, Protein Sci. 2 (1993) 522–531.
[22] J.R. Engen, D.L. Smith, Investigating protein structure and dynamics by hydrogen exchange MS, Anal. Chem. 73 (2001) 256A–265A.

[23] H. Maity, W.K. Lim, J.N. Rumbley, S.W. Englander, Protein hydrogen exchange mechanism: local fluctuations, Protein Sci. 12 (2003) 153–160.
[24] E.J. Nettleton, P. Tito, M. Sunde, M. Bouchard, C.M. Dobson, C.V. Robinson, Characterization of the oligomeric states of insulin in self-assembly and amyloid fibril formation by mass spectrometry, Biophys. J. 79 (2000) 1053–1065.
[25] R.K. Chitta, D.L. Rempel, M.A. Grayson, E.E. Remsen, M.L. Gross, Application of SIMSTEX to oligomerization of insulin analogs and mutants, J. Am. Soc. Mass Spectrom. 17 (2006) 1526–1534.
[26] S.R. Mudaliar, F.A. Lindberg, M. Joyce, P. Beerdsen, P. Strange, A. Lin, R.R. Henry, Insulin aspart (B28 asp-insulin): a fast-acting analog of human insulin—absorption kinetics and action profile compared with regular human insulin in healthy nondiabetic subjects, Diabetes Care 22 (1999) 1501–1506.
[27] A. Lindholm, J. McEwen, A.P. Riis, Improved postprandial glycemic control with insulin aspart: a randomized double-blind cross-over trial in type 1 diabetes, Diabetes Care 22 (1999) 801–805.
[28] R.H. Becker, A.D. Frick, Clinical pharmacokinetics and pharmacodynamics of insulin glulisine, Clin. Pharmacokinet. 47 (2008) 7–20.
[29] European Medicines Agency Committee for Medicinal Products for Human Use, Apidra: European Public Assessment Report—Product Information. 2011. Available from: <http://www.ema.europa.eu/docs/en_GB/document_library/EPAR_-_Product_Information/human/000557/WC500025250.pdf>.
[30] T. Heise, C. Weyer, A. Serwas, S. Heinrichs, J. Osinga, P. Roach, J. Woodworth, U. Gudat, L. Heinemann, Time–action profiles of novel premixed preparations of insulin lispro and NPL insulin, Diabetes Care 21 (1998) 800–803.
[31] M. Lepore, S. Pampanelli, C. Fanelli, F. Porcellati, L. Bartocci, A.D. Vincenzo, C. Cordoni, E. Costa, P. Brunetti, G.B. Bolli, Pharmacokinetics and pharmacodynamics of subcutaneous injection of long-acting human insulin analog glargine, NPH insulin, and ultralente human insulin and continuous subcutaneous infusion of insulin lispro, Diabetes 49 (2000) 2142–2148.
[32] G.A. Brunner, G. Sendhofer, A. Wutte, M. Ellmerer, B. Søgaard, A. Siebenhofer, S. Hirschberger, G.J. Krejs, T.R. Pieber, Pharmacokinetic and pharmacodynamic properties of long-acting insulin analogue NN304 in comparison to NPH insulin in humans, Exp. Clin. Endocrinol. Diabetes 108 (2000) 100–105.
[33] J.L. Whittingham, S. Havelund, I. Jonassen, Crystal structure of a prolonged-acting insulin with albumin-binding properties, Biochemistry 36 (1997) 2826–2831.
[34] S. Havelund, A. Plum, U. Ribel, I. Jonassen, A. Vølund, J. Markussen, P. Kurtzhals, The mechanism of protraction of insulin detemir, a long-acting, acylated analog of human insulin, Pharm. Res. 21 (2004) 1498–1504.

—Review—

再生医療製品の品質評価におけるグライコミクス

橋井則貴，中澤志織，川崎ナナ*

Glycomics in Quality Control of Tissue-engineered Medical Products

Noritaka Hashii, Shiori Nakazawa, and Nana Kawasaki*
National Institute of Health Sciences; 1-18-1 Kamiyoga, Setagaya-ku, Tokyo 158-8501, Japan.

(Received December 2, 2011)

Glycosylation of cells is known to alter with several biological events such as cell differentiations and proliferations as well as some diseases. "Glycomic approaches", comprehensive qualitative and quantitative glycan analyses of the cells, have become increasingly important as a means of discovering biomarkers that have the potential of being used as disease diagnostic markers and molecular markers for cell characterizations. In this paper, we introduce a method of quantitative glycan profiling by liquid chromatography/mass spectrometry with a combination of an isotope tagging method. In addition, we demonstrate the potential of glycan profiling as a tool for the identification of differentiated human bone marrow mesenchymal stem cell (hMSC) and non-differentiated hMSC.

Key words——glycan profiling; quantitative glycan analysis; isotope tagging method

1. はじめに

細胞に存在するタンパク質の多くは糖タンパク質であり，糖鎖部分の構造や分布は，がんや自己免疫疾患などある種の疾患，細胞分化等の生命現象，あるいは細胞環境の変化などに伴い変化することが知られている.[1-6] がん化や分化の過程で変動する糖鎖を見い出すことは，疾患の診断マーカーや細胞の分子マーカーの開発等につながる可能性がある．糖鎖は遺伝子の直接的な産物ではなく，様々な酵素反応を経て生合成される二次的産物であるため，遺伝子解析から構造や分布の変化を推定することは容易ではない．糖鎖の変化を明らかにするためには，表現型である細胞中の糖鎖を直接解析することが肝要であり，細胞糖鎖（グライコーム）の質的・量的な変化を網羅的に解析するグライコミクスに高い関心が集まっている．

グライコーム解析の手法として，レクチンを用いる方法，キャピラリー電気泳動法，質量分析法(MS)，及び蛍光標識 HPLC を用いる方法などがある.[7] これまでにわれわれは，液体クロマトグラフィー/質量分析（LC/MS）を用いた糖鎖プロファイリング法を開発し，疾患モデルマウスのグライコーム解析などに応用してきた.[8,9] 本分析法は，遊離糖鎖の還元末端を誘導体化し，グラファイトカーボンカラムを用いた LC により糖鎖を微細構造の違いで分離しながら，オンラインによる分子の質量測定，並びに多段階質量分析（MS^n）を行い，糖鎖の分布と各糖鎖の構造を推定する方法である.[9,10] 本稿では，本分析法を再生医療での応用が期待されている同種体性幹細胞のグライコーム解析に応用した例を紹介する．

2. ヒト間葉系幹細胞の糖鎖プロファイリング

ヒト幹細胞を用いる臨床研究は，臓器機能再生等を通じて国民の健康の維持並びに疾病の予防，診断及び治療に重要な役割を果たすものと考えられており，2006 年 7 月の「ヒト幹細胞を用いた臨床研究に関する指針」の施行以後，2011 年 3 月現在，28 件の臨床研究が承認されている．これらを再生医療品開発につなげるためには，品質管理の一環として，適切な生化学的指標，免疫学的指標，特徴的産生物質など適切な遺伝型あるいは表現型の指標を選択して，目的とする細胞・組織であることを確認するための手法を確立する必要がある．細胞の糖鎖は

国立医薬品食品衛生研究所（〒158-8501 東京都世田谷区上用賀 1-18-1)
*e-mail: nana@nihs.go.jp
本総説は，日本薬学会第 131 年会シンポジウム S16 で発表したものを中心に記述したものである．

がん化や分化などに伴い変化することから，目的とする細胞・組織の評価指標の1つとして利用できる可能性が高い．

Figure 1は，再生医療への応用が期待されているヒト骨髄由来間葉系幹細胞（hMSC）の糖鎖プロファイルである．hMSCは，多能性を有する体性幹細胞であり，骨，軟骨，脂肪及び神経様の細胞に分化することが知られている．[11,12] iPS細胞やhMSCなどが再生医療製品として応用可能になったとき，特性解析や品質管理等に利用できる細胞数には制限があると予想されることから，微量分析が可能な試験法の設定が求められる．LC/MSにより，わずか2×10^5個のhMSCから糖鎖分布を示すトータルイオンカレントクロマトグラム（TICC）を得ることができた．実線は，ポジティブイオンモードにより得られたTICCで，主に中性糖鎖（高マンノース型，パウチマンノース型糖鎖，混成型，及びアシアロ複合型糖鎖）の分布を示している．破線は，ネガティブイオンモードで得られたTICCで，酸性糖鎖（シアロ糖鎖）の分布を示している．Figure 1中の糖鎖構造は，各ピークに含まれる主な糖鎖の推定構造であり，MSによるフルスキャン（m/z 700–2000）で得られた分子関連イオンの質量とMS^nにより取得されたプロダクトイオンの質量から推定している．hMSCに結合している糖鎖の種類は，高マンノース型糖鎖，パウチマンノース型糖鎖，混成型糖鎖，及び複合型糖鎖と幅広く，複合型糖鎖には*N*アセチルノイラミン酸（NeuNAc）とフコース（Fuc）の結合数に不均一性がみられる．LC/MSで得られるピーク間の強度比は，糖鎖の結合比を正確には反映していないが，ピークのパターンから，中性糖鎖では高マンノース型糖鎖M8及びM9が多いこと

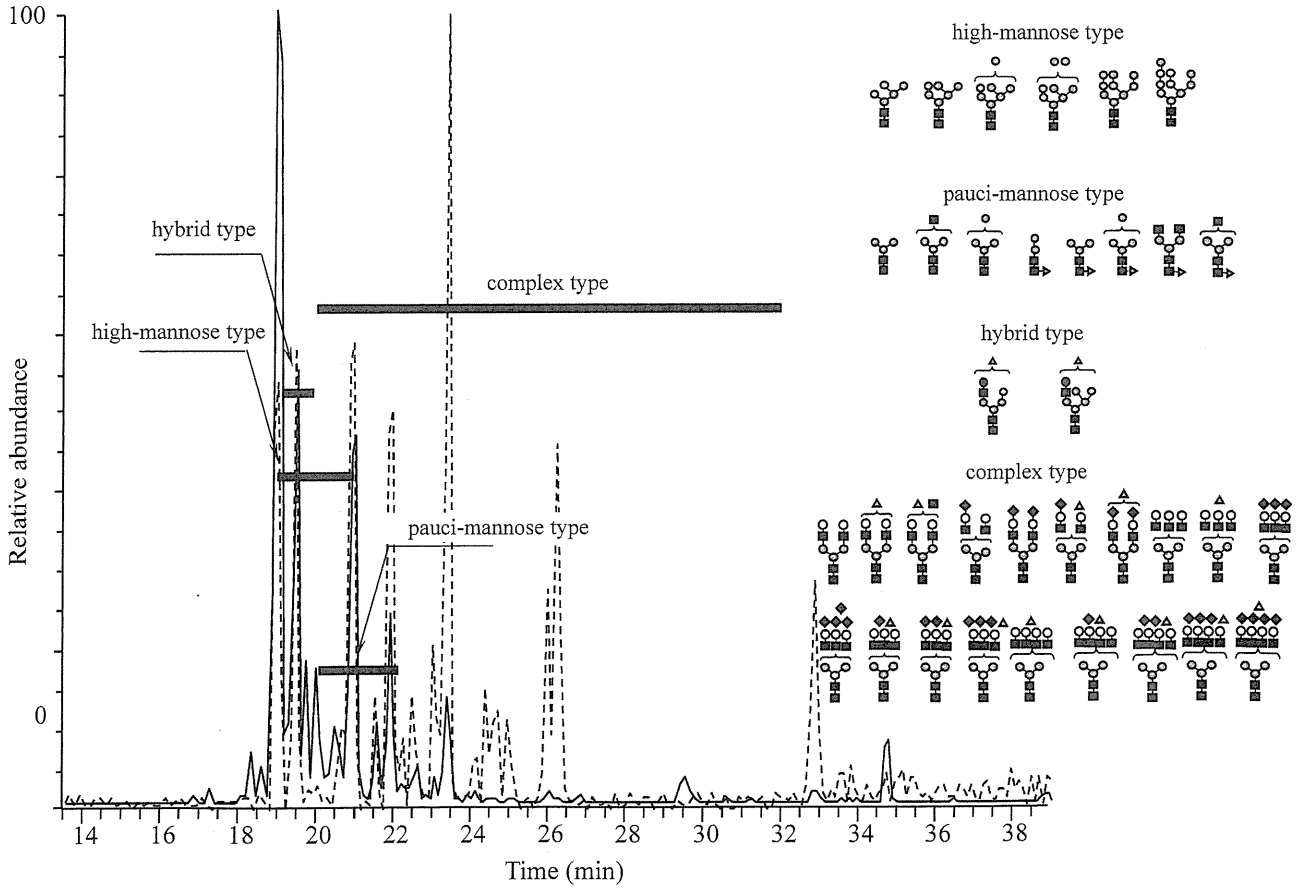

Fig. 1. Total Ion Current Chromatogram (TICC) Obtained by LC/MS of Reduced *N*-linked Glycans Prepared from hMSC

The solid line and the dashed line denote chromatograms obtained by LC/MS in the positive ion mode and the negative ion mode, respectively. LC, Paradigm MS4 HPLC system (Michrom BioResources); MS, LTQ-FT (Thermo Fisher Scientific); column, graphitized carbon column (0.075×150 mm; particle size, 5 μm); mobile phase, 5 mM ammonium bicarbonate containing 2% acetonitrile (A buffer) and 5 mM ammonium bicarbonate containing 80% acetonitrile (B buffer); flow rate, 300 nL/min; gradient condition, 2–45%B buffer (60 min); electrospray voltage, 2.5 kV in the positive and negative ion modes. △, fucose (Fuc); ●, mannose (Man); ○, galactose (Gal); ■, *N*-acetylglucosamine (GlcNAc); ◆, *N*-acetylneuraminic acid (NeuNAc).

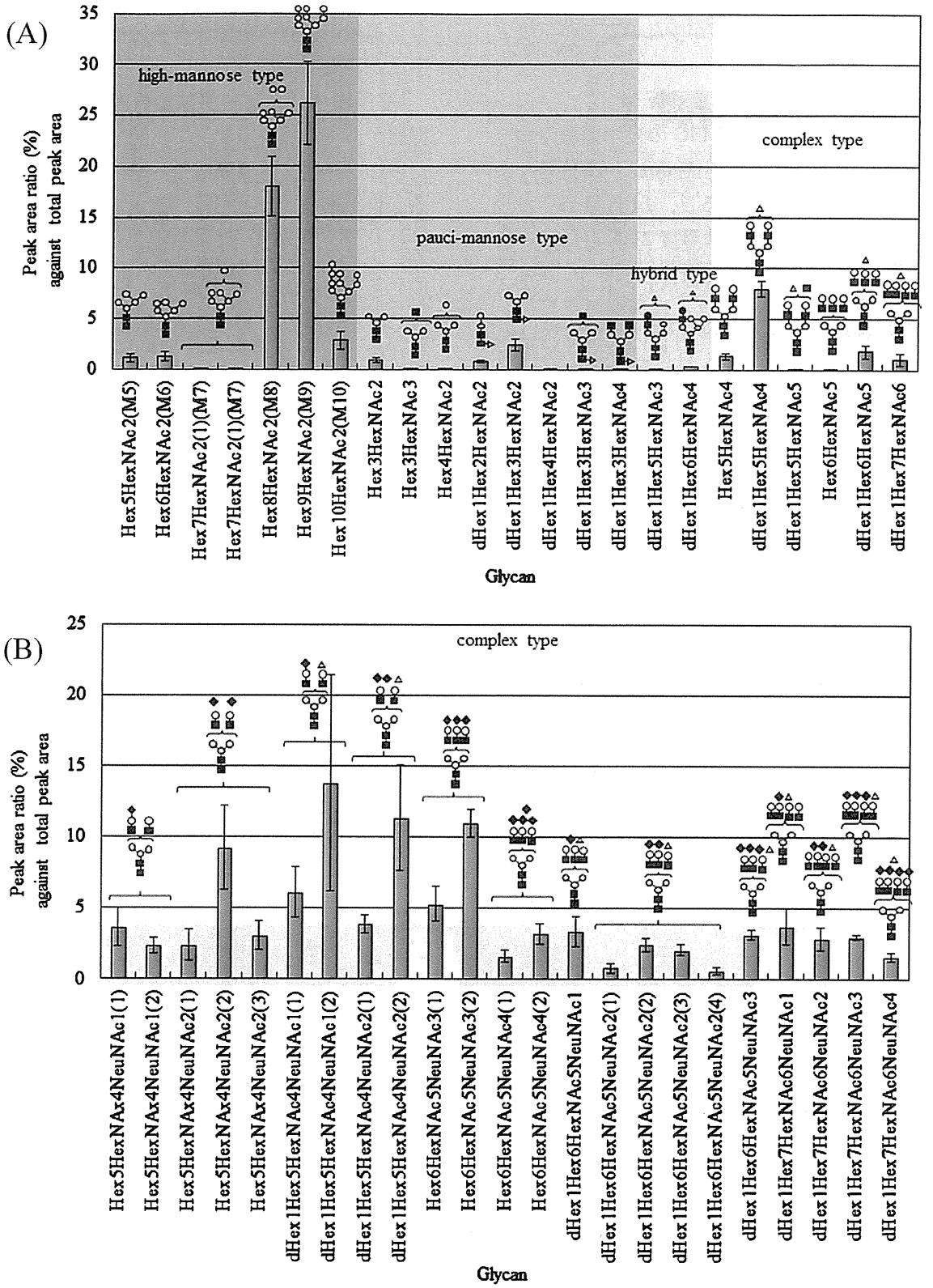

Fig. 2. Glycan Distribution in hMSC

The relative peak intensity of each glycan is expressed as a percentage of the total peak intensity of the glycans. Error bars represent the standard deviations. (A), Distribution of neutral glycans (positive ion mode); (B), distribution of sialylated glycans (negative ion mode). dHex, deoxyhexose; Hex, hexose; HexNAc, *N*-acetylhexosamine: NeuNAc, *N*-acetylneuraminic acid.

[Fig. 2(A)]，また，酸性糖鎖では，生合成後期にあらわれる分岐鎖の多い糖鎖が少ないことが示唆された［Fig. 2(B)］.

3. 細胞発現糖鎖の比較定量解析

Figure 3(A)は，未処理 hMSC の光学顕微鏡像である．hMSC を骨細胞に分化誘導し，顕微鏡により形態学的な変化を観察すると，14 日目からカルシウムの沈着が観察され，誘導後 21 日目には，細胞の約 70%にカルシウムの沈着がみられる［Fig. 3(B)］．脂肪細胞への分化では，誘導開始 7 日目から脂肪滴が観察され始め，21 日目には多くの細胞で脂肪滴の蓄積が観察される［Fig. 3(C)］．Figure 3(D)は MSC を神経様細胞に分化誘導後 2 日目の細胞であり，細胞質部分の繊維状から球状への変化，及び突起の伸長が観察され，神経細胞の形態学的な特徴を有していることがわかる．これらの分化を評価する方法として，免疫組織化学染色法やフローサイトメトリー法などにより，分化細胞に特異的に発現するタンパク質の発現の有無を確認する方法が知られている．しかし，神経様分化細胞のマーカーとして使用されているタンパク質の多くは未分化の hMSC にも発現されており，特異性に課題があることが指摘されている.[13] hMSC とその神経様分化細胞で結合量に差異が認められる糖鎖を見い出すことができれば，より特異性の高いマーカーとして利用できる可能性がある．そのためには，神経様分化前後の細胞の糖鎖分布を比較できる定量的解析手法が必要である.

LC/MS では，ピーク強度の再現性に依然として問題があり，複数のサンプル間で量的な比較を行うためには，同位体標識法や，統計的解析手法を用いる必要がある．筆者らは，重水素（D）置換 2-アミノピリジン（2AP）により調製した 4D 置換ピリジルアミノ化（PA）糖鎖を用いた比較定量法を開発している（Fig. 4）.[14] この方法は，比較する試料 A 並びに B から酵素的あるいは化学的に糖鎖を切り出し，それぞれ D 未置換 PA 糖鎖（d_0-PA 糖鎖）並びに d_4-PA 糖鎖とし，混合して LC/MS で分析する方法である［Fig. 4(A)］．d_0-PA 糖鎖と d_4-PA 糖鎖は，糖鎖部分の構造の差異に基づいて分離されるが［Fig. 4(B)］，マススペクトル上，質量 4 u 差のイオンとして分離される［Fig. 4(C)］．糖鎖量の違いはピーク強度の違いとなってあらわれるので，ピーク強度比を求めることにより，糖鎖結合比を得ることができる.

われわれの報告に続き，D 標識された 1-フェニル-3-メチル-5-ピラゾロン（PMP）や ^{13}C で標識したアラニン，2-アミノ安息香酸を用いて還元末端を標識する方法が相次いで報告された（Table 1）．また ^{13}C で標識されたヨウ化メチルで糖鎖を全メチル

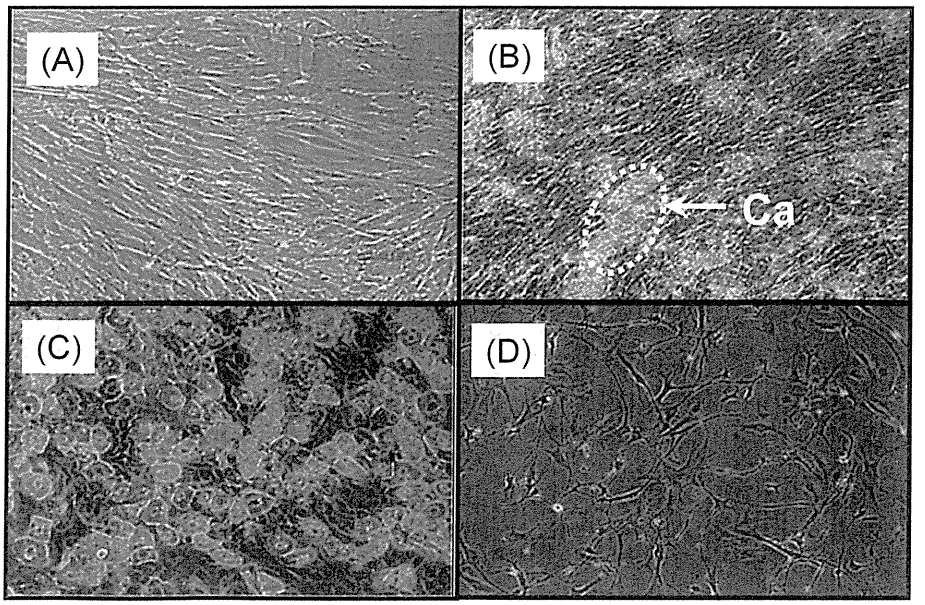

Fig. 3. Cell Images of hMSC and Its Differentiated Cells Taken by a Light Microscope
(A), hMSC; (B), osteogenic differentiation; (C), adipogenic differentiation; (D), neural differentiation.

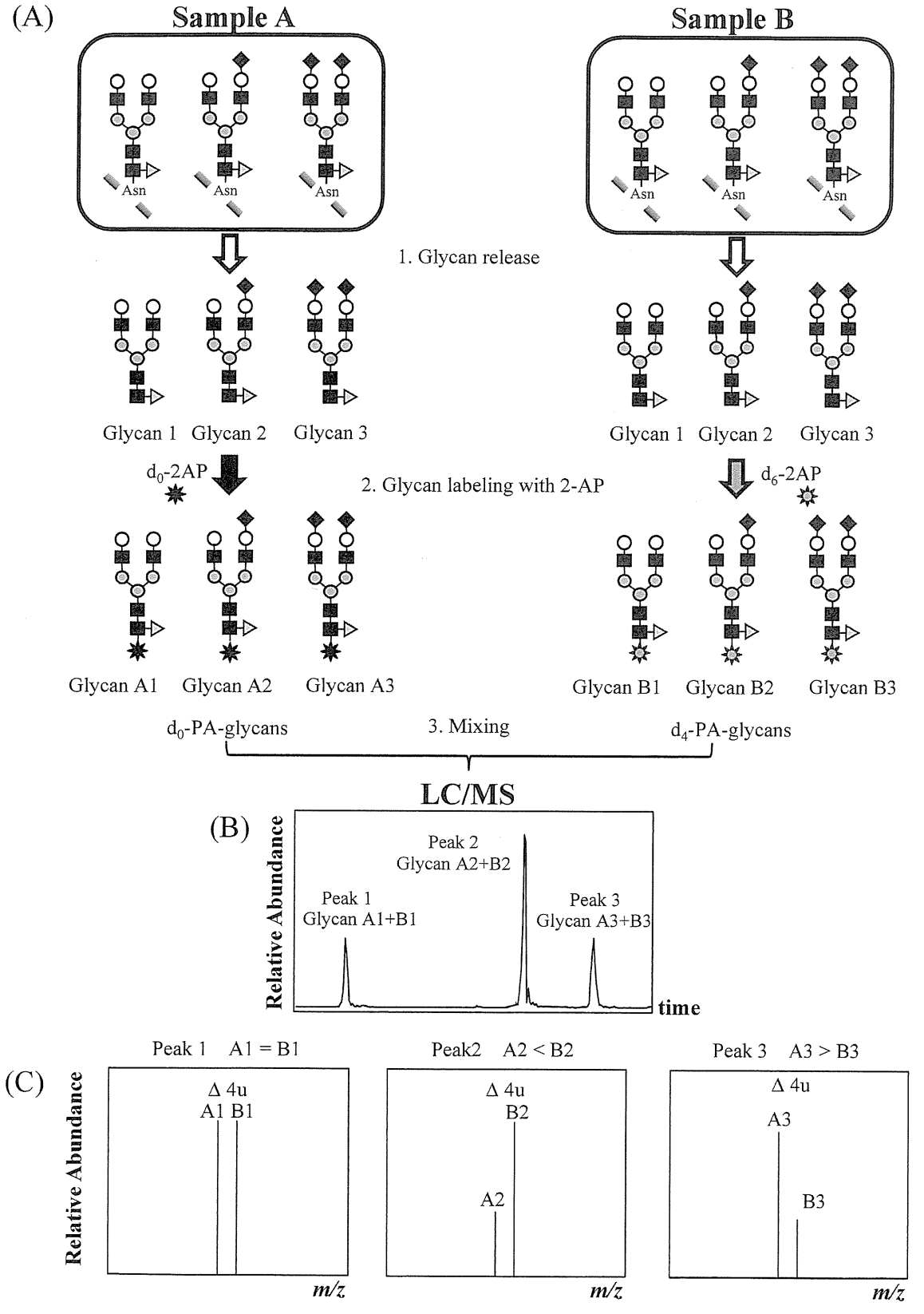

Fig. 4. Quantitative Glycan Analysis by a Combination of Isotope Tagging Method

(A), Strategy for quantitative glycan analysis using d_0-2AP and d_6-2AP as labeling reagents; (B), chromatogram obtained by the LC/MS of a mixture of d_0-PA and d_4-PA-glycans; (C), mass spectra obtained from a mixture of d_0-PA and d_4-PA-glycans.

化する方法も報告されている.[15–19] これらの方法の多くは，酸性溶液中で加熱して糖鎖を誘導体化する方法であり，シアル酸が解離する可能性があることから，シアロ糖鎖が多い hMSC には適切でない．そこでわれわれは，中性水溶液中で標識が可能なフェニルヒドラジン（PHN）を用いた，新たな糖鎖同位体標識法を開発した［Fig. 5(A)］.[21] この方法は，糖鎖試料溶液に，六炭素が ^{13}C で置換された PHN（$^{13}C_6$-PHN）塩酸塩又は未置換 PHN（$^{12}C_6$-PHN）塩酸塩，並びに還元剤 2-ピコリンボランを加えて遮光下 55℃ で 1 時間程度反応させる方法である［Fig. 5(B)］.[22,23] 反応終了後，クロロホルム抽出により，過剰な PHN 及び 2-ピコリボランを除くことができるので，標識後の後処理も簡単である．Figure 6 は，ジシアロ 2 本鎖糖鎖の $^{12}C_6$-PHN 標識体及び $^{13}C_6$-PHN 標識体の等量混合物のマススペクトルであり，m/z 1231.5 及び m/z 1234.5 に，それぞれ $^{12}C_6$-PHN 標識体及び $^{13}C_6$-PHN 標識体の 2 価イオンが観測されている．両者の質量差は 6 u であり，天然に存在する同位体の影響は少ない．

この PHN 標識法と LC/MS を用いて，未分化 hMSC と神経様に分化した hMSC の糖鎖結合量を比較定量した結果が Fig. 7 である．上向きのカラムは未分化細胞よりも神経様分化細胞で多かった糖鎖で，未分化細胞の糖鎖を 1.0 としたときの相対比，また，下向きのカラムは神経様細胞よりも未分化細胞で多かった糖鎖で，神経様分化細胞の糖鎖を 1.0 としたときの相対比を表している．hMSC を神経様細胞に分化誘導すると，Fuc 結合複合型糖鎖の高分岐化が進む一方で，3 及び 4 個の NeuNAc が結合し，かつ Fuc が結合していない複合型 3 本鎖糖鎖の割合は減少する傾向にあることがわかる．この結果は，hMSC の神経様分化において，2 日間で糖鎖のプロファイルが変わること，換言すれば，糖鎖プロファイルを比べることによって，未分化細胞と神経様分化細胞を識別できる可能性を示唆していると思われる．

4. おわりに

本稿では，再生医療での応用が期待されている hMSC を用いて，LC/MS によるグライコーム解析法が，細胞分化の評価に応用できる可能性があることを示した．これまでグラコミクスは，主にがんなどの診断マーカー探索研究の 1 つとして展開されて

Table 1. Isotope Tagging Method Using Various Reagents

Tagging reagent	Isotope	Mass difference	Solvent	Reaction temperature (℃)	Time (h)	Reducing agent	Reaction temperature (℃)	Time (h)	Sample cleanup	Reported year	Reference
2-Aminopyridine (PA)	^{2}H (D)	4	30% AcOH in DMSO	90	1	Borane-dimethylamine complex	80	1	Graphitized carbon cartridge (d)	2005	14
Aniline	^{13}C	6	30% AcOH in DMSO	65	2–4	$NaCNBH_3$	—(b)		Paper chromatography cartridge (e) Paper disk (f)	2008, 2009	15, 16
2-Aminobenzoic acid (2-AA)	^{13}C	6	2.7% AcONa, 1.3% boric acid 33% THF	80	1	$NaCNBH_3$	—(b)		Normal phase cartridge, graphitized carbon cartridge (g)	2010	17
1-Phenyl-3-methyl-5-pyrazolone (PMP)	^{2}H (D)	10	10.5% NH_3 in CH_3OH	70	1.5	—(c)			Extraction with dichloromethane	2011	20
Permethylation	^{13}C	—(a)	DMSO	<25	>4	—(c)			Extraction with chloroform	2007	18, 19

(a), Mass difference between ^{13}C-labeled sample and ^{12}C-labeled sample changes depending on glycan; (b), amination and reduction were performed by a one-step process; (c), reduction is not performed; (d), Envi-Carb (Supelco); (e), GlycoClean S (Prozyme); (f), 3-MM paper filter (Whatman); (g), normal phase DPA-6S PhyTips and Carbo-pack tips (PhyNeous).

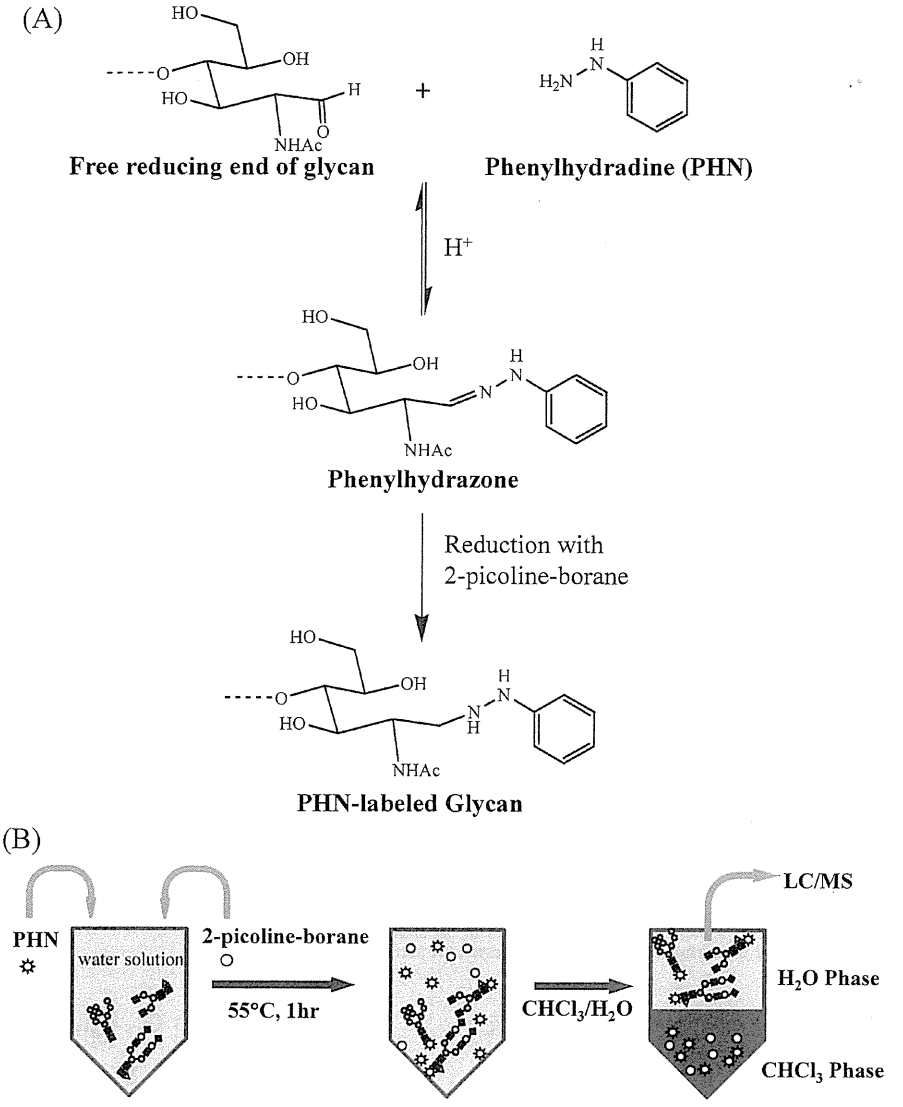

Fig. 5. Tagging of Glycan with Phenylhydrazine (PHN)
(A), Reaction mechanism of glycan tagging with PHN; (B), preparation of PHN labeled glycan.

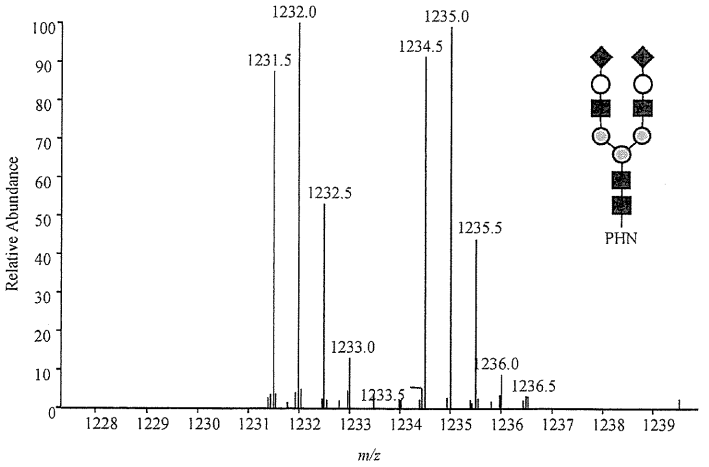

Fig. 6. Mass Spectrum of a Mixture of $^{12}C_6$-PHN and $^{13}C_6$-PHN Labeled Disialylated Core-fucosylated Complex Type Biantennary

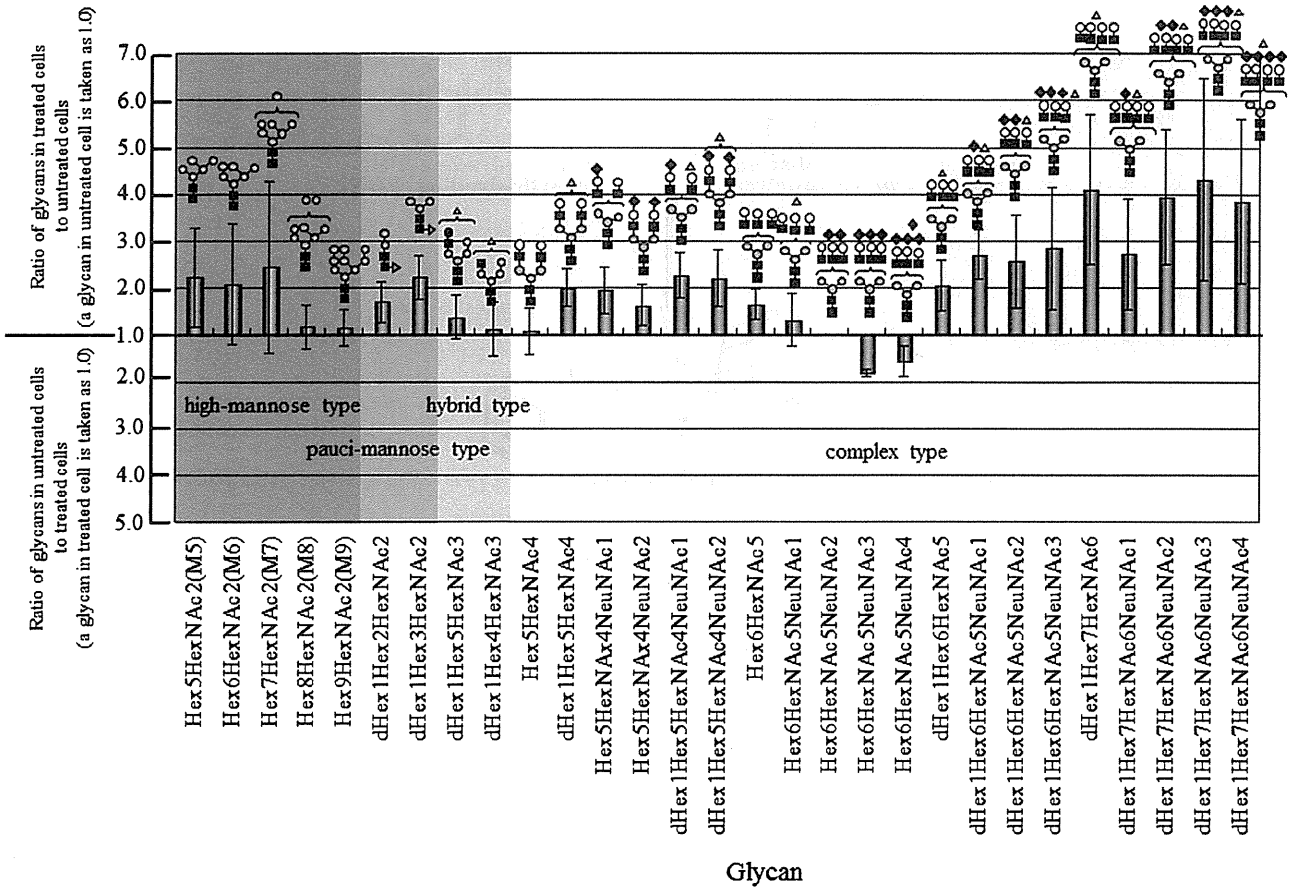

Fig. 7. Quantitative Glycan Analysis between hMSC (untreated cell) and Its Neural-lineage Cell (treated cell)
Each value is the average of a triplicate. Error bars represent the standard deviations.

きたが，それらの研究を通して確立された様々な技術が，今後，再生医療製品の品質管理手法の1つとしても発展していくことが期待される．

謝辞　本研究は，厚生労働科学研究費補助金並びに科学研究費補助金若手（B）の研究成果の一部である．

REFERENCES

1) Feizi T., Gooi H. C., Childs R. A., Picard J. K., Uemura K., Loomes L. M., Thorpe S. J., Hounsell E. F., *Biochem. Soc. Trans.*, **12**, 591–596 (1984).
2) Kannagi R., Izawa M., Koike T., Miyazaki K., Kimura N., *Cancer Sci.*, **95**, 377–384 (2004).
3) Lau K. S., Partridge E. A., Grigorian A., Silvescu C. I., Reinhold V. N., Demetriou M., Dennis J. W., *Cell*, **129**, 123–134 (2007).
4) Heiskanen A., Hirvonen T., Salo H., Impola U., Olonen A., Laitinen A., Tiitinen S., Natunen S., Aitio O., Miller-Podraza H., Wuhrer M., Deelder A. M., Natunen J., Laine J., Lehenkari P., Saarinen J., Satomaa T., Valmu L., *Glycoconj. J.*, **26**, 367–384 (2009).
5) Miyoshi E., Shinzaki S., Moriwaki K., Matsumoto H., *Methods Enzymol.*, **478**, 153–164 (2010).
6) Hossler P., Khattak S. F., Li Z. J., *Glycobiology*, **19**, 936–949 (2009).
7) Hirabayashi J., Kuno A., Tateno H., *Electrophoresis*, **32**, 1118–1128 (2011).
8) Hashii N., Kawasaki N., Itoh S., Nakajima Y., Kawanishi T., Yamaguchi T., *Immunology*, **126**, 336–345 (2009).
9) Hashii N., Kawasaki N., Itoh S., Hyuga M., Kawanishi T., Hayakawa T., *Proteomics*, **5**, 4665–4672 (2005).
10) Itoh S., Kawasaki N., Hashii N., Harazono A., Matsuishi, Hayakawa T., Kawanishi T., *J. Chromatogr. A*, **1103**, 296–306 (2006).
11) Prockop D. J., *Science*, **276**, 71–74 (1997).

12) Sanchez-Ramos J., Song S., Cardozo-Pelaez F., Hazzi C., Stedeford T., Willing A., Freeman T. B., Saporta S., Janssen W., Patel N., Cooper D. R., Sanberg P. R., *Exp. Neurol.*, **164**, 247–256 (2000).
13) Tondreau T., Lagneaux L., Dejeneffe M., Massy M., Mortier C., Delforge A., Bron D., *Differentiation*, **72**, 319–326 (2004).
14) Yuan J., Hashii N., Kawasaki N., Itoh S., Kawanishi T., Hayakawa T., *J. Chromatogr. A*, **1067**, 145–152 (2005).
15) Xia B., Feasley C. L., Sachdev G. P., Smith D. F., Cummings R. D., *Anal. Biochem.*, **387**, 162–170 (2009).
16) Lawrence R., Olson S. K., Steele R. E., Wang L., Warrior R., Cummings R. D., Esko J. D., *J. Biol. Chem.*, **283**, 33674–33684 (2008).
17) Prien J. M., Prater B. D., Qin Q., Cockrill S. L., *Anal. Chem.*, **82**, 1498–1508 (2010).
18) Alvarez-Manilla G., Warren N. L., Abney T., Atwood J. 3rd, Azadi P., York W. S., Pierce M., Orlando R., *Glycobiology*, **17**, 677–687 (2007).
19) Kang P., Mechref Y., Kyselova Z., Goetz J. A., Novotny M. V., *Anal. Chem.*, **79**, 6064–6073 (2007).
20) Zhang P., Zhang Y., Xue X., Wang C., Wang Z., Huang L., *Anal. Biochem.*, **418**, 1–9 (2011).
21) Lattova E., Perreault H., *J. Chromatogr. B Analyt. Technol. Biomed. Life Sci.*, **793**, 167–179 (2003).
22) Sato S., Sakamoto T., Miyazawa E., Kikukawa Y., *Tetrahedron*, **60**, 7899–7906 (2004).
23) Ruhaak L. R., Steenvoorden E., Koeleman C. A., Deelder A. M., Wuhrer M., *Proteomics*, **10**, 2330–2336 (2010).